Colloid Polym Sci 276:999–1009 (1998)
© Steinkopff Verlag 1998

ORIGINAL CONTRIBUTION

N. Girard
Th.F. Tadros
A.I. Bailey

Polymerization of oil (styrene and methylmethacrylate)-in-water microemulsions

Received: 29 May 1997
Accepted: 28 May 1998

N. Girard · Dr. Th.F. Tadros (✉)
ZENECA Agrochemicals
Jealott's Hill Research Station
Bracknell
Berkshire RG12 6EY
UK

I. Bailey
Department of Chemical Engineering
and Chemical Technology
Imperial College of Science
Technology and Medicine
Prince Consort Road
London SW7 2BY
UK

Abstract The polymerization of styrene-in-water and methylmethacrylate-in-water microemulsions stabilized by nonionic surfactants was investigated using different initiation techniques. Thermally induced initiation was carried out using potassium persulfate (water soluble) and azobisiso-butyronitrile (AIBN) (oil soluble) at 60° and 50 °C, respectively. When the monomer concentration was kept below a certain limit, the particle size of the nanolatex was similar to the droplet size of the microemulsion precursor. At higher monomer concentrations, the latex produced was significantly larger than the microemulsion droplets, as a result of the possible coalescence of the microemulsion droplets during polymerization. By using chemically induced polymerization (hydrogen peroxide + ascorbic acid) at temperatures below the cloud point temperature of the microemulsion or by photochemically induced initiation at room temperature, it was possible to obtain nanolatex particles with similar size to the droplets up to 10% monomer content. In all cases, the particle size was determined using photon correlation spectroscopy (PCS). Electron micrographs of the microlatex particles were taken and these confirmed the measurements obtained by PCS. The molecular weight of the polymers produced was determined by gel permeation chromatography. The average number of polymer molecules per particle was calculated. It was shown in some cases that the nanolatex contained one polymer chain per particle. A mechanism was suggested for polymerization and particle growth.

Key words Microemulsions – polymerization – nanolatex

Introduction

In recent years, there has been considerable interest in the polymerization of microemulsions for various industrial applications [1–3]. Some of the most comprehensive investigations in this field have been carried out by Candau et al. [4–6] who studied the polymerization of water-in-oil (w/o) microemulsions containing acrylamide monomer in the aqueous droplets. The objective of this work was to prepare polyacrylamide with high molecular weight for application in enhanced oil recovery. The size of the nanolatex produced was larger than that of the water droplets of the microemulsion. Candau et al. [7, 8] suggested a mechanism to explain the reason for the increase in size during polymerization. As a result of the droplet collision, they may undergo fusion by coalescence resulting in larger particles after polymerization. The polymer produced was of higher molecular weight than that produced in aqueous polymerization and it was suggested that the polymer chains are relatively compressed in the core of the water droplets. However, on dilution of the nanolatex with water, inversion took place and the polyacrylamide readily dispersed and dissolved in the aqueous phase producing a highly viscous solution that is suitable for application in enhanced oil recovery.

Investigations on the polymerization of oil-in-water (o/w) microemulsions were relatively scarce. However, El-Aasser et al. [9, 10] studied the polymerization of styrene-in-water microemulsions using a mixture of an ionic surfactant and long-chain alcohol. However, the nanolatices produced were larger in size than those of the microemulsion droplet precursor. We have also recently investigated the polymerization of styrene-in-water and methylmethacrylate-in-water microemulsions [11]. These systems were prepared using nonionic surfactants and a small amount of anionic surfactant. The nanolatices produced were always larger than the size of the droplets of the monomer precursor. A mechanism similar to that suggested by Candau et al. [8, 9] was suggested to account for the increase in size. The particle size of the resulting nanolatices was measured using photon correlation spectroscopy (PCS) and their stability against flocculation by electrolyte investigated using PCS and turbidity. This work made a starting point for detailed investigations of the polymerization of o/w microemulsions and this is the objective of the present paper. A systematic study of the polymerization of styrene-in-water and methylmethacrylate-in-water microemulsions was carried out using various initiation methods. The conditions were carefully adjusted to see whether the size of the microemulsion droplet could be maintained. The resulting nanolatex was characterized using PCS and transmission electron microscopy. The molecular weight of the polymer produced was also determined using gel permeation chromatography. It was possible to produce nanolatex particles with comparable size to the microemulsion droplets from which they were produced. These results led to a change in the thinking of the mechanism of microemulsion polymerization.

Experimental

Materials

All materials were the same as described before [12]. Styrene and methylmethacrylate monomers were obtained from BDH and used as received. The nonionic surfactants were nonylphenol polyethylene oxide with 4 and 15 moles of ethylene oxide (Synperonic NP4 and NP15, respectively). They were supplied by ICI Surfactants and used as received. Aerosol OT (dioctyl sulphosuccinate) was obtained from Aldrich and purified as described before [12]. Sodium dodecyl benzene sulfonate (NaDBS) was supplied by Albright and Wilson. Potassium persulphate (98% purity), azobisisobutyronitrile (97% purity) and hydrogen peroxide (30% w/v) were purchased from BDH, ascorbic acid (99% purity) from Rhone-Poulenc. Water was doubly distilled using an all glass apparatus.

Polymerization procedure

The o/w microemulsions were prepared using the inversion method [12]. The polymerization reaction was thermally, photochemically initiated (using both water and oil soluble initiators) or chemically initiated (redox reaction). The water soluble initiator (potassium persulphate: $K_2S_2O_8$) was introduced in to the microemulsion after its preparation. The oil soluble initiator (azobisisobutyronitrile: AIBN) was introduced into the oil phase before the formation of the microemulsion. The initiator concentrations were between 10^{-4} and 10^{-1} mol dm^3. The $K_2S_2O_8$ concentration was expressed as the number of moles per unit volume of microemulsion whereas the AIBN concentration was expressed as number of moles per unit volume of monomer. The chemical initiation was carried out through a redox reaction between ascorbic acid (2.5×10^{-3} g per g monomer) and hydrogen peroxide (H_2O_2, 2.5×10^{-2} g per g monomer); both were introduced simultaneously, into the water continuous phase, just before the polymerization. The thermally and chemically induced polymerizations were carried out using a three-necked round bottom flask fitted with a condenser, a thermometer and a stopper. The flask containing the microemulsion was immersed into an oil bath. The system was then brought to the reaction temperature (60 °C for $K_2S_2O_8$ initiation, 50 °C for AIBN initiation and 30–45 °C for the redox initiation) using a hot plate and constantly mixed using a magnetic stirrer. The reaction was carried out over 24 h (thermal initiation) or 4 h (chemical initiation), the temperature was controlled with an accuracy of ±1 °C. The photochemically induced polymerization was carried out at 20 °C, over 4 h, using a double jacketed quartz vessel with circulating water. A 125 W low-pressure mercury vapor lamp was used as a source for UV radiation.

Nanolatex characterization

Photon correlation spectroscopy

The PCS instrument was the same as described before [12]. Initially, results were obtained as a function of the volume fraction of the latex and the results extrapolated to infinite dilution to obtain the hydrodynamic diameter,

$$D = D_o(1 + \alpha\phi)\ , \quad (1)$$

where D is the collective (apparent) diffusion coefficient of the particles at a volume fraction ϕ, D_o is the diffusion coefficient of single particles and α is the repulsive interaction parameter [13]. Using the Stokes-Einstein equation ($D = kT/6\pi\eta R$, where k is the Boltzmann constant, T the absolute temperature, η is the viscosity of the medium and R is the hydrodynamic radius), Eq. (1) can be written in the form

$$\frac{R_o}{R_{app}} = 1 + \alpha\phi\ , \quad (2)$$

where R_{app} is the apparent radius that is calculated without taking into account the interaction between the particles and R_o is the real particle diameter. A typical plot of R_{app}/R_o versus ϕ is shown in Fig. 1. A straight line is obtained with a slope equal to 1.5 as predicted from theory. The extrapolated value of R_o is larger than R_{app} and dilution of the latex ten times or more did not cause any further increase in the particle radius. It was then decided to use a dilution of ten times for all systems produced carrying out the PCS measurements.

Transmission electron microscopy (TEM)

Electron micrographs were taken using a Phillips microscope model 3DG, operated at 80 kV. The objective aperture was normally 30 μm. The magnification was calibrated against a diffraction grating replica (within an accuracy of ±5%). A negative staining technique using phosphotungstic acid (PTA) was applied to the samples before observation.

Gel permeation chromatography

The polymer was precipitated in an excess of cold ethanol [14]. It was then recovered by filtration, washed several times with hot water and dried in an oven at 50 °C. The molecular weight determination was carried out using a 60 cm column from Polymer Laboratories which was fitted into a Knauer 60 cm column oven. The column was calibrated to cover the molecular weight range 580–1 030 000. Tetrahydrofuran was used as the eluent, at a flow rate of 1 ml min^{-1} (Knauer 64 HPLC pump). The detector at the end of the column was a Viskotech DV200 differential refractometer/viscometer. A universal calibration curve was created using narrow polystyrene standards from Polymer Laboratories. The polymer samples were diluted to a concentration of 5 mg ml^{-1}; they were allowed to stand for atleast 4 h, filtered through a 0.45 μm membrane and injected into the column using a Gynkotek Gina Autosampler. Both weight average, M_w, and number average, M_n, were determined. The polydispersity of the polymer is given by the ratio M_w/M_n.

Results and discussion

Thermally induced polymerization

With styrene monomer two initiators, namely, $K_2S_2O_8$ (water soluble) and AIBN (oil soluble), were used. Figure 2

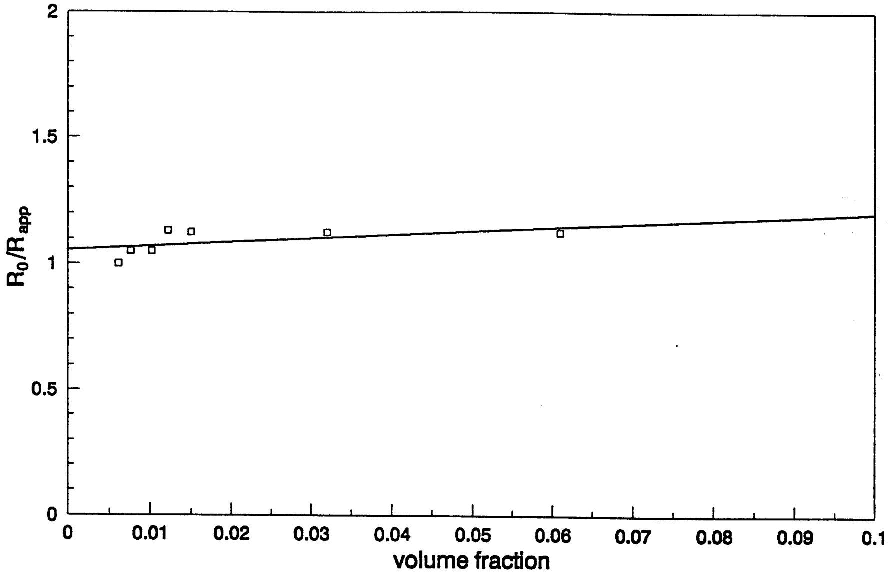

Fig. 1 R_0/R_{app} as a function of volume fraction for a polystyrene latex dispersion

Fig. 2 Variation of particle diameter after polymerization of styrene-in-water microemulsions, using $K_2S_2O_8$ at 60 °C

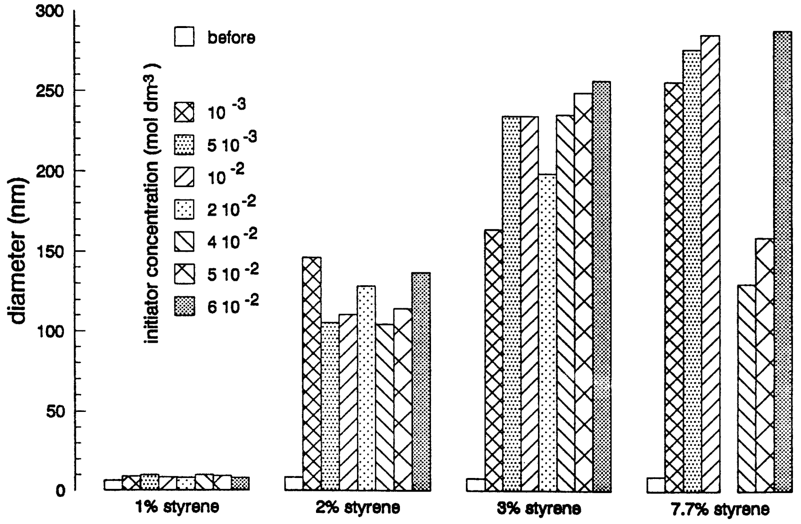

Fig. 3 Variation of particle diameter after polymerization of styrene-in-water microemulsions, using AIBN at 50 °C

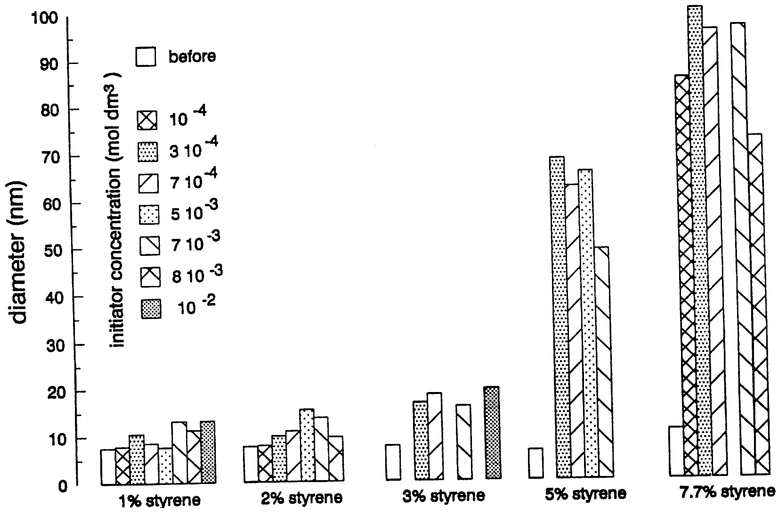

shows a summary of the droplet diameters produced at various $K_2S_2O_8$ concentrations and monomer contents. There was a small effect of initiator concentration on the final particle size, but there was significant effect of the monomer content. In this case, particle diameters comparable to those of the droplet size of the microemulsions were only obtained at low styrene content (<2%). For example at 1% styrene nanolatices were obtained with a diameter in the region 8–10 nm, whereas those of the microemulsions were about 6 nm. Above this styrene level, the particle diameter was several orders of magnitude higher than that of the microemulsion (see Fig. 2).

Figure 3 shows a summary of the results using AIBN. In this case, the particle diameters were comparable to those of the microemulsion droplets up to 2% styrene, above which they started to become larger. However, at 3% styrene the nanolatex diameter was only about twice the size of the initial droplets. This difference between AIBN and $K_2S_2O_8$ may be accounted for as a result of the difference in the reaction temperature in the two cases. With $K_2S_2O_8$, the reaction temperature was 60 °C, which is above the cloud point temperature of the system [12], particularly at >1% styrene. As discussed before [12], above the cloud temperature of the system, the microemulsion becomes unstable and there is a rapid increase in droplet size. In addition, there is a difference in the initiation processes between $K_2S_2O_8$ and AIBN. In the former case, initiation takes place at the surface of the microemulsion droplet since the initiator molecules diffuse from the bulk aqueous phase to the surface of the droplet. This may accelerate the coalescence process. On the other hand, with AIBN, initiation starts in the oil phase, since the molecules are present in that phase and this may slow down the coalescence process. In both cases, there was little dependence of the particle diameter on the initiator concentration and this could be due to the fast polymerization reaction. Similar results were previously obtained by Larpent and Tadros [11] using 7% styrene and $K_2S_2O_8$ as the initiator.

Gan et al. [15] also produced latex particles using ionic surfactants and alchohol cosurfactant, although they kept the temperature at 40 °C, their particles were large (20–100 nm).

Guo et al. [10] produced latices of the order of 20–30 nm using 5% styrene and similar surfactant system as that used by Gan et al. Thus all results, including those reported in the present paper show that thermally induced polymerization is not a good method for producing latices of size comparable to that of the microemulsion droplets.

Chemically induced polymerization

Only styrene-in-water microemulsions were investigated, the concentration of ascorbic acid and H_2O_2 was kept constant (see experimental section), while varying the reaction temperature. Figure 4 shows a summary of the particle diameters obtained at various styrene contents and various temperatures. It can be seen from this figure that there is little dependence of the particle diameter on the styrene content up to 11.6% and the reaction temperature (within the range 30–45 °C). In addition, the particle diameter only increases by 1–3 nm above the diameter obtained for the microemulsion precursor. The polydispersity indices of all the resulting latices were relatively high (~0.3) and similar to those of the microemulsion precursor. This high polydispersity index makes it difficult to differentiate between the various samples. The small size latex produced may be due to the shorter reaction time (4 h) and the lower temperature (<45 °C) when compared with those of thermally induced polymerization (see previous section).

Photochemically induced polymerization

In this case both styrene and MMA microemulsions were investigated using AIBN and UV (see experimental section). Figure 5 shows the results for the polystyrene microlatices produced, whereas Fig. 6 shows the corresponding results for polymethylmethacrylate microlatices. Figure 5A shows that when the styrene content was lower than 9%, there was little dependence of particle diameter on AIBN concentration until 10^{-2} mol dm^{-3}, above which there was a monotonic increase in size with further increase in initiator concentration. At 12% styrene, this monotonic increase started at 10^{-3} mol dm^{-3} AIBN. Figure 5B shows that below 9% styrene, the particle

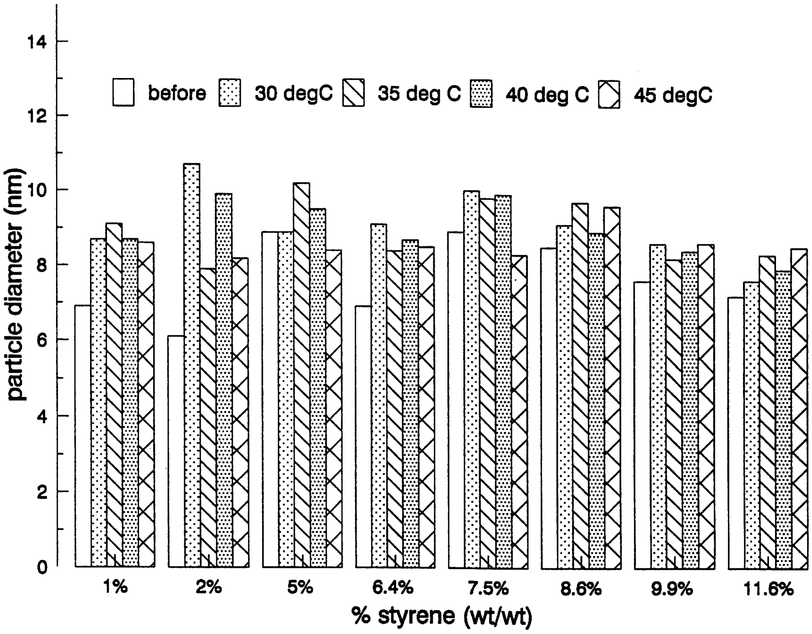

Fig. 4 Variation of particle diameter after polymerization of styrene-in-water microemulsions, using ascorbic acid and H_2O_2

Colloid & Polymer Science, Vol. 276, No. 11 (1998)

Fig. 5 (A) Variation of particle diameter, after UV polymerization of styrene-in-water microemulsions, using AIBN concentration. (B) Variation of particle diameter, after UV polymerization of styrene-in-water microemulsions, with styrene concentration

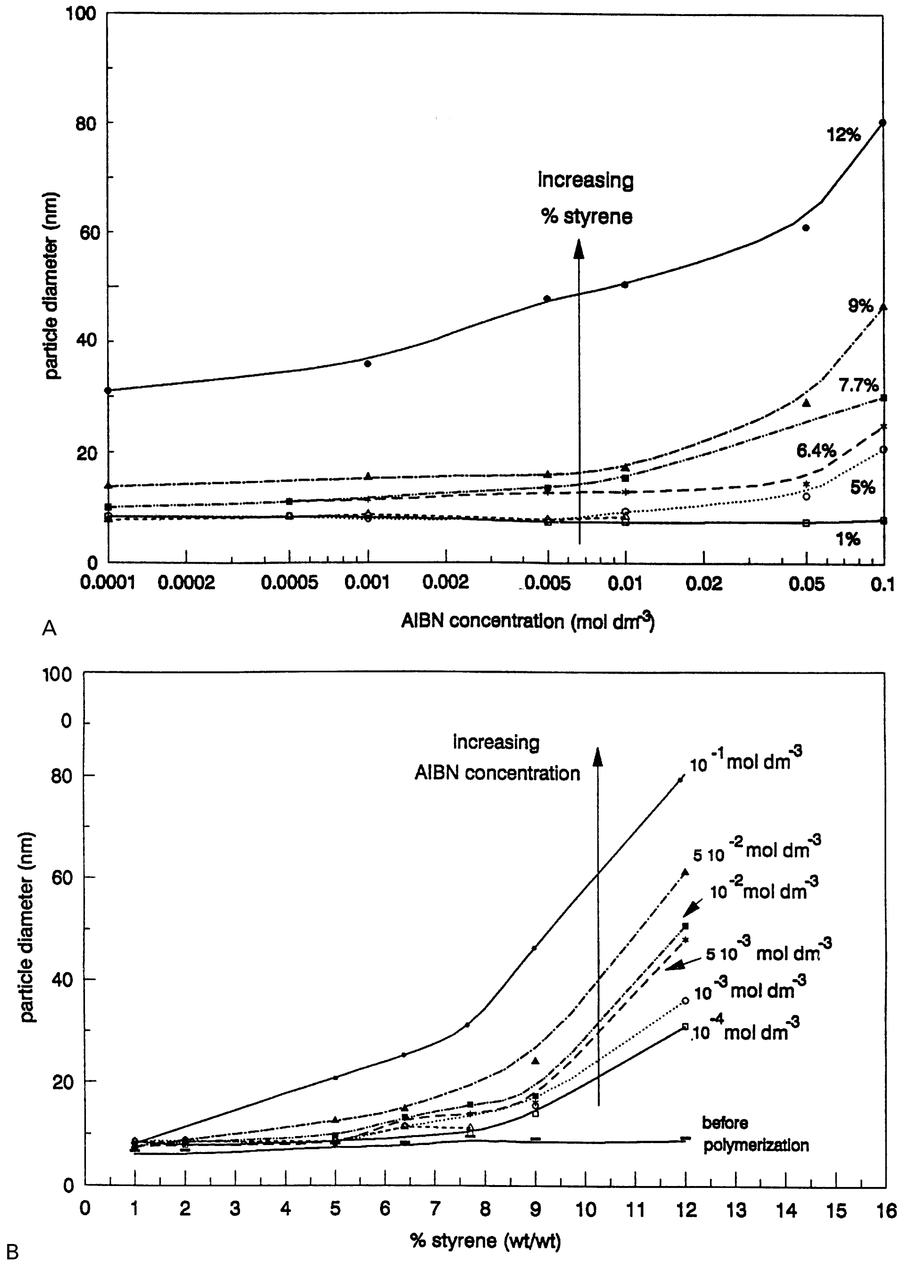

diameter increases only slightly above the values for the microemulsion droplets provided the initiator concentration is kept below 5×10^{-2} mol dm^{-3}. Above 9% styrene, the particle diameter shows a rapid increase with further increase in styrene content.

The corresponding results using MMA show similar trends to styrene, indicating that by using AIBN and UV one is able to prepare particles with similar sizes to those of the microemulsion droplets up to ~10% by controlling the initiator concentration. At higher monomer concentration, the latex size obtained increased but was still below 50 nm up to 12% styrene and 14% MMA (provided the initiator concentration was kept below 5×10^{-2} mol dm^{-3}). These results are consistent with the lower temperatures at which the polymerization reactions were carried out when using UV. In all cases the temperature was always below 25 °C and this was well below the cloud temperature of the microemulsion system. These conditions reduced the possibility of significant coalescence of the microemulsion droplets during polymerization. However, if the initiator

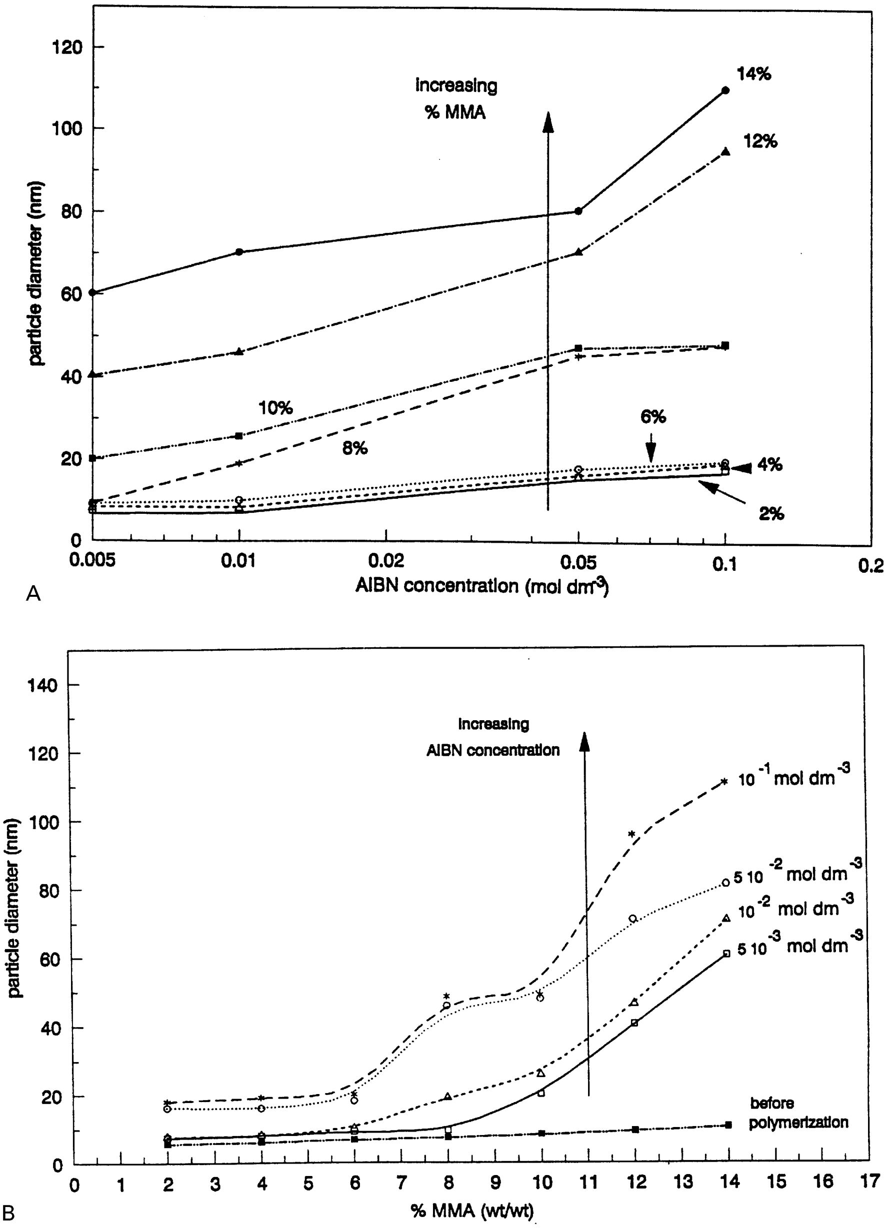

Fig. 6 (A) Variation of particle diameter, after UV polymerization of MMA-in-water microemulsions, with AIBN concentration. (B) Variation of particle diameter, after UV polymerization of MMA-in-water microemulsions, with MMA concentration

concentration was significantly increased, the rate of production of free radicals increases resulting in the growth of the particles (see below).

Transmission electron microscopy results

Figure 7 shows typical electron micrographs of polystyrene latices obtained by thermal polymerization. Figure 7a shows the result for 1% styrene and 10^{-2} mol dm^{-3} $K_2S_2O_8$ and a reaction temperature of 60 °C. At higher initiator concentrations, the latex flocculated during the staining process and, therefore, it was difficult to obtain any micrographs. The results in Fig. 7a show clearly the polydispersity value of 0.24. However, the electron micrograph confirms that the average diameter obtained by PCS gives a reasonable estimate of the microlatex size. Figure 7b and c shows the micrographs for polystyrene microlatex (at 2 and 3% styrene, respectively) prepared using AIBN (10^{-2} mol dm^{-3}) as initiator and at a temperature of 50 °C. These micrographs show similar sizes to those obtained using $K_2S_2O_8$ initiator at 1%

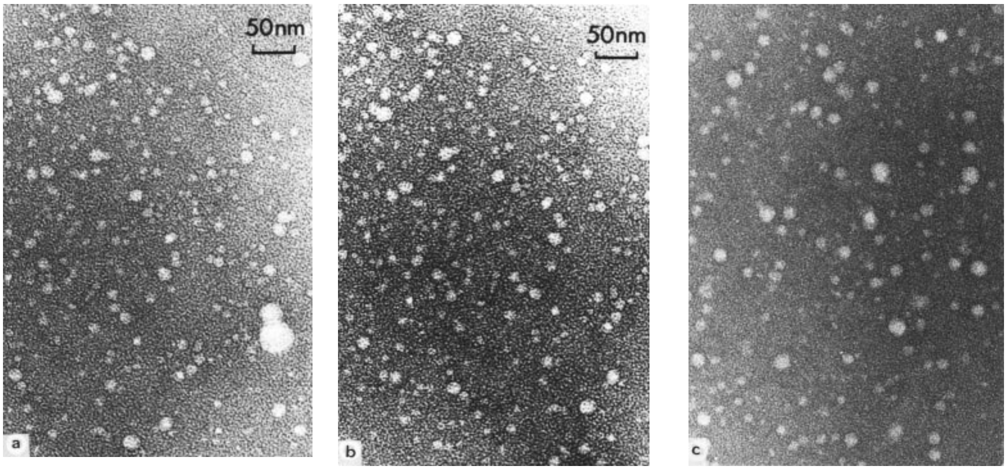

Fig. 7 Electron micrographs of microlatices: (a) 1 wt/wt% styrene, polymerization – 10^{-2} mol dm^{-3} $K_2S_2O_8$ at 60 °C (PCS results – $d = 10$ nm; polydispersity = 0.24); (b) 2 wt/wt% styrene, polymerization – 10^{-2} mol dm^{-3} AIBN at 50 °C (PCS results – $d = 9.5$ nm; polydispersity = 0.25); (c) 3 wt/wt% styrene, polymerization – 10^{-2} mol dm^{-3} AIBN at 50 °C (PCS results – $d = 11.3$ nm; polydispersity = 0.25)

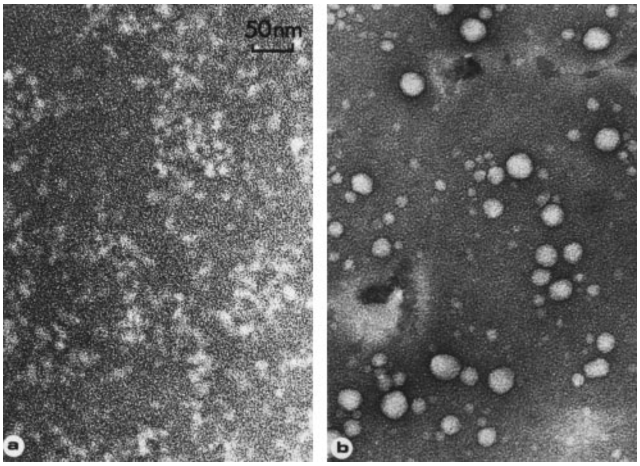

Fig. 8 Electron micrographs of polymethylmethacrylate nanolatices: (a) 2 wt/wt% MMA, polymerization – 10^{-2} mol dm^{-3} AIBN using UV (PCS results – $d = 10.1$ nm; polydispersity = 0.22); (b) 8 wt/wt% MMA, polymerization – 10^{-2} mol dm^{-3} AIBN using UV (PCS results – $d = 25.1$ nm; polydispersity = 0.30)

styrene content (Fig. 7a). The PCS results gave diameters of 9.5 nm (polydispersity 0.25) and 11.3 nm (polydispersity 0.25) at 2 and 3% styrene, respectively. Again the electron micrographs are in qualitative agreement with the PCS results.

Figure 8 shows the corresponding results for the chemically induced polymerization process for 1 and 6% styrene at 40 °C (concentration of hydrogen peroxide and ascorbic acid was kept constant at 2.5×10^{-2} and 2.5×10^{-3} g per g monomer). The photomicrographs illustrate the polydispersity and confirm the size obtained by PCS (9.6 and 10.6 nm for 1 and 6% styrene, respectively).

Figure 9 shows photomicrographs for UV polymerization and AIBN initiator for polystyrene at various concentrations of styrene. The results show that by increasing the styrene content, while keeping the initiator concentration constant, the particle size increases (see Fig. 9c and d). On the other hand, if the styrene content is kept constant, then increasing the initiator concentration results in an increase in the particle size (see Fig. 9b and d). This is consistent with the higher rate of production of free radicals with increase in initiator concentration (see below).

Figure 10a and b shows two micrographs for PMMA lattices obtained at a monomer concentration of 2 and 8%, respectively using UV and a constant AIBN concentration of 10^{-2} mol dm^{-3}. As with styrene, increasing the MMA content results in an increase in the particle size.

Molecular weight results

Table 1 shows a summary of the results of the molecular weight determined by GPC. All results show that the polymers are polydisperse giving a ratio of M_w/M_n greater than 3. Determination of the free monomer concentration in the latex after polymerization showed a value lower than 1%. This means that the entire volume of the latex particles is occupied by the polymer molecules. In this case it is possible to calculate the average number of molecules, n, per particle from the average radius, r, i.e.,

$$n = \frac{4\pi r^3 \rho_{PS} N_A}{3 M_w} , \qquad (3)$$

where ρ_{PS} is the density of polystyrene which was taken to be 1.05 and N_A is the Avogadro's constant.

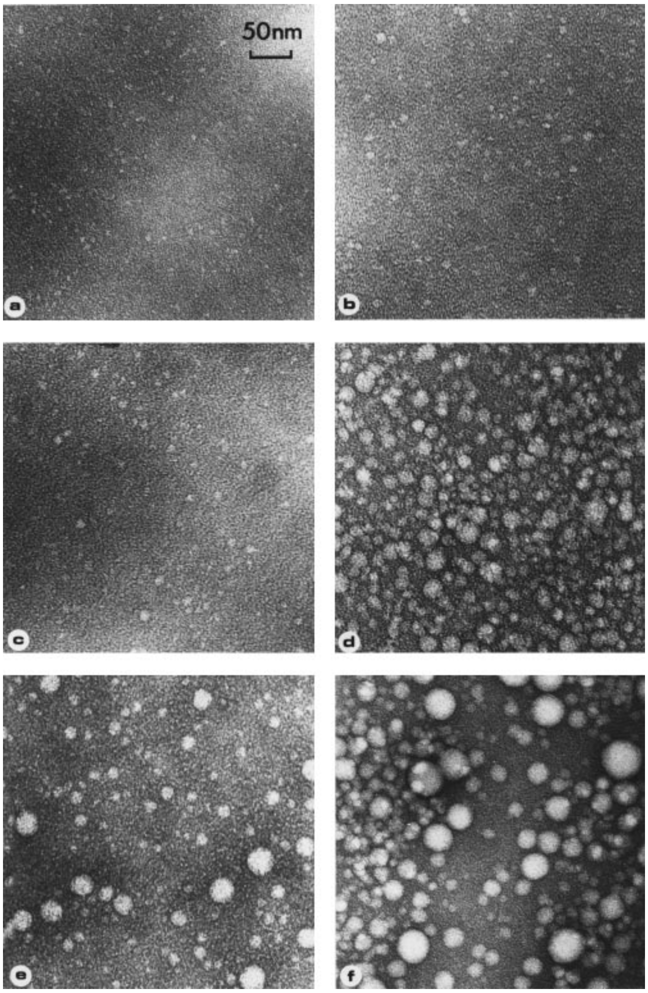

Fig. 9 Electron micrographs of polystryrene nanolatices: (a) 1 wt/wt% styrene, polymerization 10^{-1} mol dm^{-3} AIBN using UV (PCS results – $d = 8.1$ nm; polydispersity = 0.19); (b) 5 wt/wt% styrene, polymerization 5×10^{-2} mol dm^{-3} AIBN using UV (PCS results – $d = 8.5$ nm; polydispersity = 0.18); (c) 6 wt/wt% styrene, polymerization 5×10^{-2} mol dm^{-3} AIBN using UV (PCS results – $d = 8.6$ nm; polydispersity = 0.21); (d) 5 wt/wt% styrene, polymerization 10^{-1} AIBN using UV (PCS results – $d = 21.0$ nm; polydispersity = 0.26); (e) 9 wt/wt% styrene, polymerization – 5×10^{-2} mol dm^{-3} AIBN using UV (PCS results – $d = 24.1$ nm; polydispersity = 0.28); (f) 11 wt/wt% styrene, polymerization 10^{-3} mol dm^{-3} AIBN using UV (PCS results – $d = 30.2$ nm; polydispersity = 0.29)

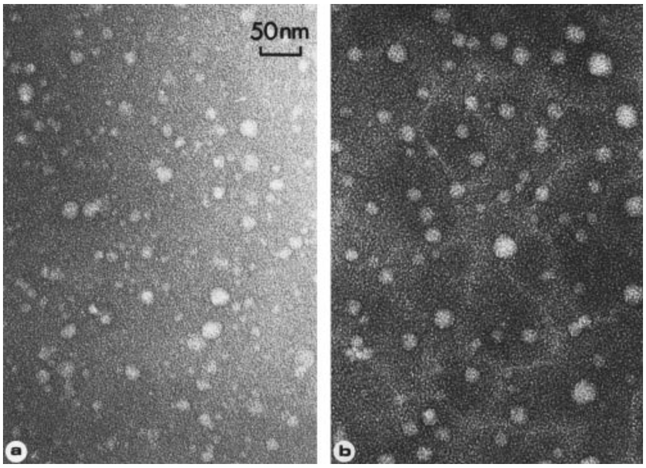

Fig. 10 Electron micrographs of polystryrene nanolatices: (a) 1 wt/wt% styrene, polymerization ascorbic acid/H_2O_2 at 40 °C (PCS results – $d = 9.6$ nm; polydispersity = 0.35); (b) 6 wt/wt% styrene, polymerization ascorbic acid/H_2O_2 at 40 °C (PCS results – $d = 10.6$ nm; polydispersity = 0.35)

The results for the UV polymerized styrene with AIBN initiator shows an average value of between 1.6 and 11.6. This means that in some cases, 1–2 molecules per particle are produced. Since the average radius was taken to be the hydrodynamic radius, which is greater than the core radius, it is likely that in some cases there will be only one polymer molecule per particle.

The limited results for the chemically induced polymerization of styrene (Table 1b) and the UV polymerization of MMA (with AIBN initiator) show similar trends to those obtained for UV polymerized styrene.

Polymerization mechanism

The above results showed without doubt that the polymerization of styrene or methylmethacrylate in an oil-in-water microemulsion depends strongly on the temperature at which the polymerization is carried out. If that temperature is below the cloud point temperature of the microemulsion, the polymerization occurs in a continuous manner within the droplet, possibly by a diffusion process (mechanism I) as illustrated in Fig. 11. Due to the dynamic equilibrium between the droplets in a microemulsion [16], there will be exchange of monomer as well as initiator molecules. This would result in a continuous polymerization process which can take place at a very fast rate so that only one molecule may be produced per particle. This mechanism explains the reason for the formation of nanolatex particles with the same size as the initial microemulsion droplet and the possibility of producing one chain per particle. It is also possible for the particles to grow by diffusion of monomer molecules through the continuous phase. In this case, the particle size will be larger than the microemulsion droplet size but only by a factor not exceeding two. In contrast to this mechanism, there is the possibility of collision between the microemulsion droplets and their coalescence resulting in a much larger increase in the particle size. This is illustrated in Fig. 12. This latter mechanism (II) is preferred when the

Table 1

(*a*) *Molecular weight of polystyrene obtained by UV polymerization*

% Styrene [wt/wt]	AIBN Conc. [mol dm^{-3}]	d/nm	M_w/M_n	$M_w/10^4$	$M_n/10^4$	n
5	5×10^{-3}	7.6	3.7	6.63	1.77	1.9
5	5×10^{-2}	9.5	3.1	7.52	2.41	3.7
5	10^{-1}	23.8	3.2	44.50	13.80	9.0
5	10^{-1}	26.2	3.4	51.0	11.5	11.6
6.4	5×10^{-3}	13.8	3.1	31.0	9.95	2.8
6.4	10^{-2}	12.2	5.8	35.2	6.1	1.6
6.4	5×10^{-2}	7.8	4.2	4.1	0.97	3.8
6.4	10^{-1}	8.6	4.0	2.77	0.68	7.5
7.7	10^{-2}	24.9	5.6	120	21.4	4.2
9	10^{-2}	27.8	5.4	93.1	17.0	7.6
9	10^{-2}	17.4	5.6	74.9	13.3	2.3
9	5×10^{-2}	25.8	4.6	77.0	16.6	7.4
11.6	10^{-2}	33.0	6.6	192	29.0	6.1

(*b*) *Molecular weight of polystyrene obtained by polymerization using ascorbic acid and H_2O_2 at 40 °C*

wt/wt% polystyrene	d/nm	M_w/M_n	$M_w/10^4$	$M_n/10^4$	n
1	8.7	2.3	4.225	1.872	2.0
5	9.5	3.5	2.323	0.664	3.7
6.4	8.7	3.0	5.939	2.019	9.9

Fig. 11 Diffusion mechanism of polymerization

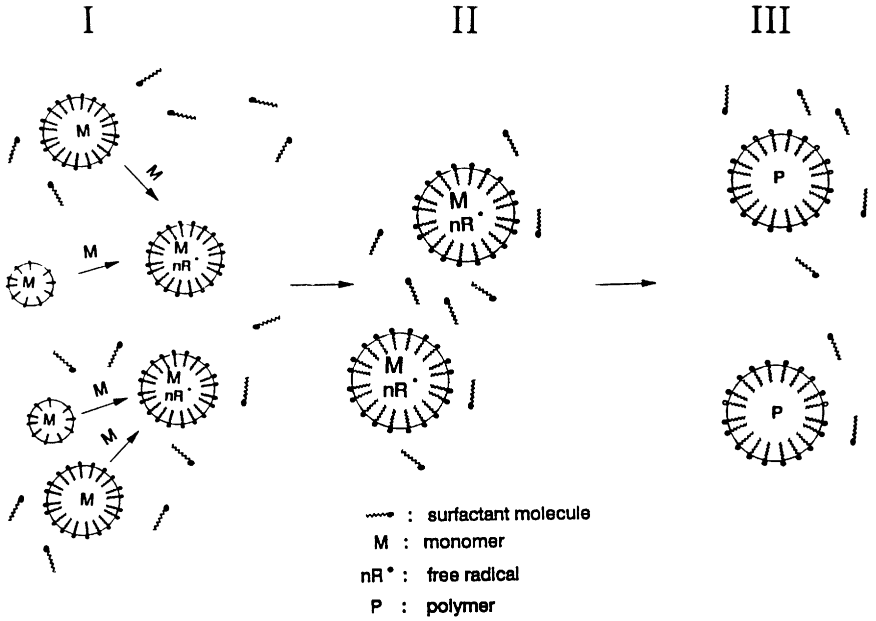

polymerization occurs at a higher temperature or at high monomer content. Near and above the cloud temperature of the microemulsion system, collision between the droplets is facilitated enhancing the possibility of growth by the second mechanism.

The polymerization was also dependent on the initiator concentration. If the latter is kept below a certain limit, the production of free radicals does not occur at a fast rate. In this case, the polymerization takes place by mechanism I and the particle size will be comparable to that of the droplet size of the microemulsion precursor, provided the monomer content is sufficiently low to prevent any collision between the droplets. On the other hand, if the initiator concentration is relatively high, the rate of production of free radicals increases. Many monomer droplets are therefore initiated and many growing free radicals (polymerizing polymer chain) are produced over a very short period of time (nucleation period). In addition,

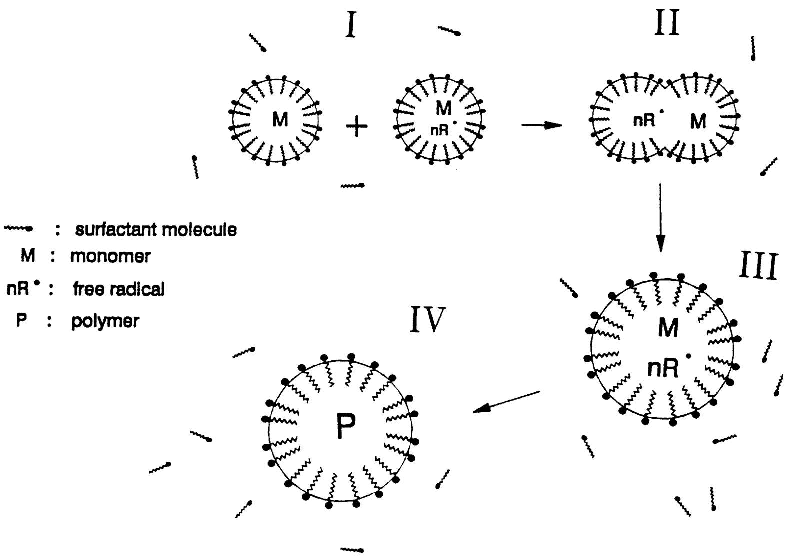

Fig. 12 Collision mechanism of polymerization

the probability for a free radical to penetrate a droplet is higher when the droplet already contains a free radical [17]. The greater the amount of initiator in the droplets, the higher the probability for the polymerizing free radicals to meet another free radical molecule. Because of the small volume of the latex particles, the entering free radical will react with the polymer free radical by termination rather than initiating a new chain. A microemulsion droplet containing a terminated polymer chain is unlikely to be easily initiated again (the termination rate is much faster than the initiation rate) and will consequently act as a monomer reservoir for the other polymerizing droplets, using the remaining unpolymerized monomer molecules. As a consequence, the number of monomer droplets acting as reservoirs is higher when the initiator concentration is increased, resulting in the particle growth. A similar particle growth with increase of initiator concentration is usually observed with emulsion polymerization [18].

Conclusions

In this paper we have demonstrated for the first time that nanolatex particles with similar size to those of the microemulsion precursor could be obtained by controlling the polymerization conditions. This could be obtained using nonionic surfactants for microemulsion preparation. The reaction temperature should be kept below the cloud temperature of the microemulsion, while maintaining the monomer content and the initiator concentration below a certain limit. This ensures that the polymerization takes place in a continuous manner in the droplets. In certain cases, one polymer molecule per particle may be produced. As the monomer content and/or initiator concentration is increased, particle growth may take place by collision between the droplets during polymerization. At high initiator concentrations, the rate of production of free radicals is greatly enhanced and this leads to larger particles.

References

1. Atik SS, Thomas JK (1981) J Am Chem Soc 103:4280
2. Candau F (1990) Makromol Chem Makromol Symp 31:27
3. Stoffer JO, Bone T (1980) J Dispersion Technol 1:37
4. Durand JP, Nicolas D, Kohler N, Dawans F, Candau F (1987) French patent (to IFP), 2 565 623
5. Durand JP, Nicolas D, Kohler N, Dawans F, Candau F (1987) French patent (to IFP), 2 565 592
6. Durand JP, Nicolas D, Candau F (1987) French patent (to IFP), 2 567 525
7. Leong YS, Candau F (1982) J Phys Chem 86:2269
8. Candau F, Leong YS, Candau G, Candau S (1985) In: Degiorgi V, Corti M (eds) Progr SIF Course XV, p 830
9. Kuo PL, Turro NJ, Tseng CM, El Aasser MS, Vanderhoff JW (1987) Macromolecules 20:1216
10. Guo JS, El Aasser MS, Vanderhoff JW (1989) J Polym Sci Polym Chem 27:691
11. Larpent C, Tadros ThF (1991) Colloid Polym Sci 269:1171
12. Girard N, Tadros ThF, Bailey AI (1997) Colloid Polym Sci
13. Cazabet AM, Langevin D (1981) J Chem Phys 74:3148
14. Rabagliati FM, Falcon AC, Gonzales DA, Martin C, Anton RE, Salager JL (1986) J Disp Sci Technol 7:245
15. Gan LM, Chew CH, Lye I, Imae T (1991) Polym Bull 25:193
16. Fletcher PDI, Howe AM, Robinson BH (1987) J Chem Soc Faraday Trans I 83:985
17. Alexander AE, Napper DH (1971) Progr Polym Sci 3:145
18. Chamberlain BJ, Napper DH, Gilbert RG (1982) J Chem Soc Faraday Trans I 78:591